Imaging the dynamics of dyke propagation prior to the 2000-2003 flank eruptions at Piton de La Fournaise, Reunion Island

A. Peltier, V. Ferrazzini, T. Staudacher, P. Bachèlery

Imaging the dynamics of dyke propagation prior to the 2000–2003 flank eruptions at Piton de La Fournaise, Reunion Island

A. Peltier,[1,2] V. Ferrazzini,[2] T. Staudacher,[2] and P. Bachèlery[1]

[1]   The relationship between shallow magma storage and flank injections in volcanic edifices is rarely documented. We analyse the time series of geodetic and seismic data collected at Piton de La Fournaise volcano (La Reunion) during 9 flank eruptions from 2000 to 2003. The data depicts how magma injections supplied flank eruptions at Piton de la Fournaise volcano, and allows to precisely determine the direction and duration of dike intrusions, indicating a two phases pattern, consistent over all the eruptions: 1) Fast vertical migration of the dyke ($\sim$2 m/s) from the magma chamber to the surface in 10 to 50 minutes, and 2) slower, lateral migration (0.2–0.8 m/s) in tens of minutes to hours controlled by the rift zone geometry. **Citation:** Peltier, A., V. Ferrazzini, T. Staudacher, and P. Bachèlery (2005), Imaging the dynamics of dyke propagation prior to the 2000–2003 flank eruptions at Piton de La Fournaise, Reunion Island, *Geophys. Res. Lett.*, *32*, L22302, doi:10.1029/2005GL023720.

1.   Introduction

[2]   Modeling the geometry of dyke intrusion leading to an eruption has important bearing on the risk assessment on volcanoes. Some recent models applied to Kilauea (Hawaii) [*Cervelli et al.*, 2002], Etna (Sicilia) [*Bonaccorso et al.*, 2002] and Piton de La Fournaise (PdF) (La Reunion, Indian Ocean) [*Battaglia and Bachèlery*, 2003; *Froger et al.*, 2004; *Fukushima et al.*, 2005] volcanoes have determined the final shape of dykes within the edifice, based on surface displacements recorded by GPS, continuous tilt, or deduced from ASAR interferometry. Most often, these models deduced from punctual data do not provide any constraints on the dynamics of dyke propagation itself owing to the lack of continuous record of motions during its emplacement.

[3]   At Piton de la Fournaise (PdF) most of the eruptions occur within the Enclos Fouqué caldera that encloses the cone-shaped central edifice (Figure 1). In few cases (1977, 1986, and 1998) flank eruptions occur outside of the caldera, and represent a potential threat for the populations. It is therefore necessary to monitor in real time the dynamics of dyke migration, and predict the possible location of flank eruptions. *Toutain et al.* [1992] calculated the migration of the inflation centre from tilt signals preceding the 1990 eruption. It is, however, a major interest to combine the available data of numerous volcanic crisis, in order to constrain the dynamics of dyke injection. We analyse here continuous recording of tiltmeter and seismic data during the most recent eruptions (2000–2003) of PdF volcano. The data allow a precise description and chronology of the magma injection process, from the rupture of the chamber's roof to the propagation of the dyke at the origin of the eruption. Our results provide a better understanding of eruptive mechanisms at PdF and can be used as a tool for a risk assessment in real time.

[4]   Over 11 effusive eruptions have taken place at PdF from 2000 to 2003. We focus on 9 flank eruptions that occurred inside the Enclos Fouqué caldera, along two rift zones oriented N10°E and N170°E, and along a broad eruption axis oriented N120°E (Figure 1 and Table 1). The two remaining eruptions (May and December 2003) were limited to the summit of the volcano inside the Dolomieu crater, and are not considered here.

2.   Methods

[5]   Since 1980, the Volcanological Observatory of Piton de la Fournaise (OVPF) monitors the activity of the PdF using telemetered instruments including (i) tiltmeters and (ii) permanent seismic stations (Figure 1).

[6]   (i) The tiltmeter network of the OVPF is composed of six stations recording with a frequency of 1 sample/min (Figure 1); three of them are located around the summit craters and the three others at the base of summit cone. Each of these stations is composed of two Blum-type pendulum tiltmeters, orientated radially and tangentially to the summit. Tiltmeters are sensitive to diurnal temperature variations (a few tens of μrad). We corrected the intrusive signals (several hundreds of μrad) from these daily variations by subtracting the record of a quiet day having a similar temperature profile. The combination of the movement recorded by the two tiltmeters, radial and tangential, gives us, as function of time, the direction and intensity of the real tilt. Figure 2 shows these tilt vectors describing the slope movement due to the inflation source. The vectors point away from inflation source, and allow us to evaluate the displacement of the inflation centre with time (Figure 3). The location of the source of inflation is geometrically computed as the barycentre of the tilt vectors supplied by the six stations. Due to the lack of stations at the base of the central cone, it is not possible to follow the migration of the inflation centre outside of the network.

[7]   (ii) The seismic network consists in 20 stations (Figure 1) equipped with short-period geophones (1 Hz) recorded continuously with a frequency of 100 samples/sec. In order to visualise the dyke propagation and the opening of the eruptive fissures, we compare the seismic background noise (bgn) on different stations. The seismic bgn is the root

[1]Laboratoire des Sciences de la Terre (UMR7154), Université de la Réunion, Saint-Denis, France.
[2]Observatoire Volcanologique du Piton de la Fournaise (UMR7154), Institut de Physique du Globe de Paris, La Plaine des Cafres, France.
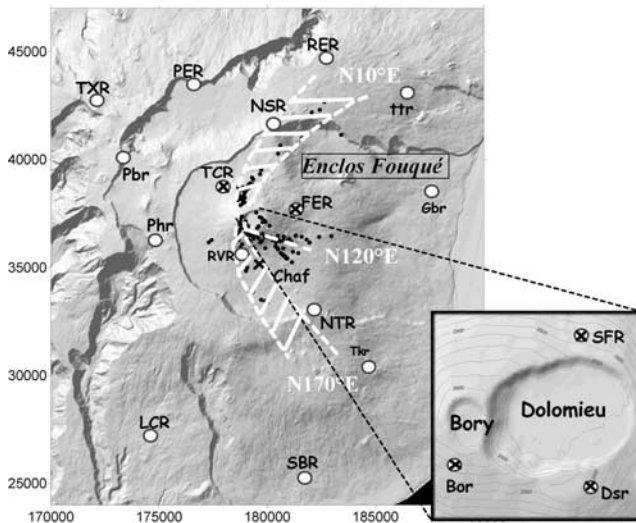
Figure 1. Structural map of Piton de la Fournaise volcano. The rift zones are indicated by white dash lines. The black crosses, white dots, and black dots indicate the location of respectively tiltmeters, seismic stations, and eruptive vents from 1998 to 2003.

mean square of the seismic signal amplitude calculated for each minute over one minute.

3. Results and Interpretation

3.1. Pre-Eruptive Pattern of Flank Eruptions

[8] For 9 flank eruptions we analyse the tilt and seismic data, and compare the migration of the inflation centre as a function of time. For each of them, the tilt radial components steadily increased indicating inflation of the summit, before apparition of clear signals related to the start of the intrusion to the flank. Thus we can distinguish initial upwards movement of magma (phase 1) and the near-surface lateral expansion to the eruption site (phase 2).

[9] In the first phase, the seismic crisis starts with a considerable seismic bgn centred below the summit craters (up to 100 μm/s) (Figure 4). The seismic swarm is located in a well identified zone on the border of the Dolomieu crater at a level ranging between 200 to 800 m above sea level (see Figure 6).
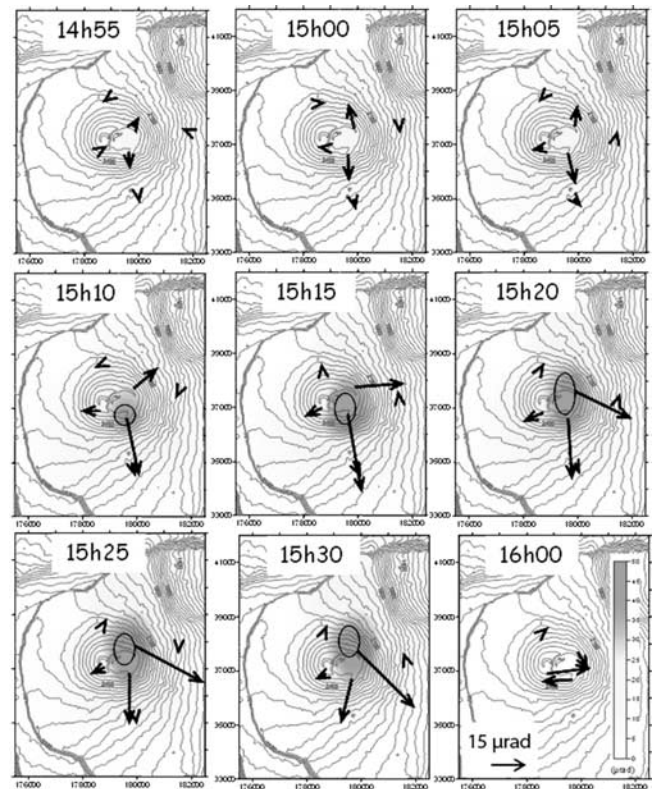

Figure 2. August 2003 dyke intrusion. The maps show the tilt variations observed within a 5 minutes time window, from 14h50 to 15h30. The last map shows the tilt variations between 15h30 and 16h00. Vectors point away from inflation source. Color scale represents contours of deformation amplitude. See color version of this figure in the HTML.

[10] A few minutes (5 to 10) after the beginning of the seismic crisis, tiltmeters record the first signs of summit inflation. The intensity of the tilt increases and the direction of vectors stabilises, defining an inflation centre in the vicinity of the Dolomieu crater. These data indicate that the first motion of magma out of the reservoir is vertical (Figures 2 and 3) and located below Dolomieu crater. The tilt stations record up to 1000 μrad at the summit, while the stations on the flank usually only show variations of about

Table 1. Summary of 2000–2003 Eruptions

Date of Eruption[a]	Location	Altitude of the Eruptive Fissure, m	Seismic Crisis Duration, min[b]	Vertical Injection Duration, min[c]	Lateral Injection Duration, min[d]
14-Feb-00	north flank	2450–2250	64	22	39
23-June-00	east flank south-east	2100–1820	72	23	43
12-Oct-00	south-east flank	2260–2000	57	15	34
27-March-01	south flank south-east	2450–1940	26	7	13
11-June-01	south-east flank	2450–1800	32	10	20
05-Jan-02	north-east flank	1910–1070	383	32	346
16-Nov-02	east flank	1850–1500	296	35	253
22-August-03	Bory + north flank	2590–2140	152	20	125
30-Sept-03	west flank south-west	2330–2195	65	13	42

[a]The reader is referred to the Bulletin of the Global Volcanism Network website (www.volcano.si.edu) for a more extensive phenomenological description of each eruption.

[b]Considering the time between the beginning of the seismic swarm and the opening of the first eruptive fissure.

[c]From the beginning of the summit inflation to the beginning of the lateral displacement of the inflation centre.

[d]From the lateral displacement of the inflation centre to the opening of the first eruptive fissure.
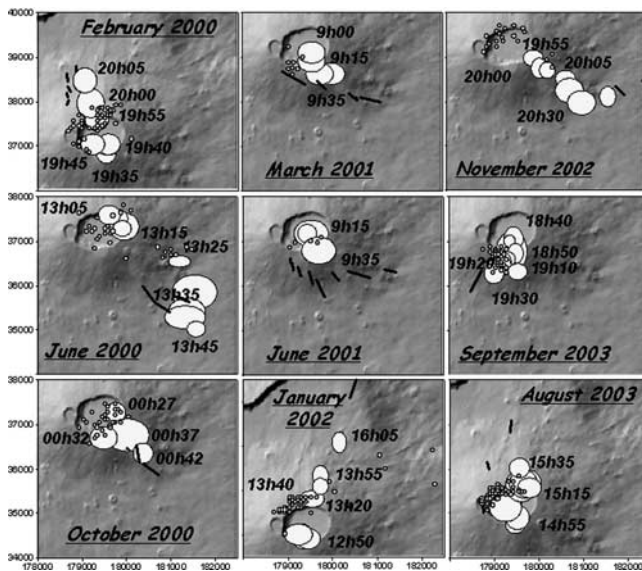
Figure 3. Migration of inflation centres for the 9 eruptions from 2000 to 2003, as estimated from tilt data. Small circles and black lines indicate respectively the location of earthquakes and the eruptive fissures.

10 μrad, indicating a source of deformation shallower than 3 km depth [*Lénat and Bachèlery*, 1990]. More precisely, from one event to another, different settings of this inflation centre may be distinguished (Figure 3). For the eruptions of Feb. 2000, Jan. 2002, Aug. and Sept. 2003, the first inflation centre is located in the south-western part of Dolomieu crater. The alternation of eruption on the northern and southern flanks agrees with the model of *Lénat and Bachèlery* [1990] and the existence of a very shallow storage system above sea level consisting of several magma pockets. Following this model, each eruption is triggered by a single magma pocket. Another explanation could be the
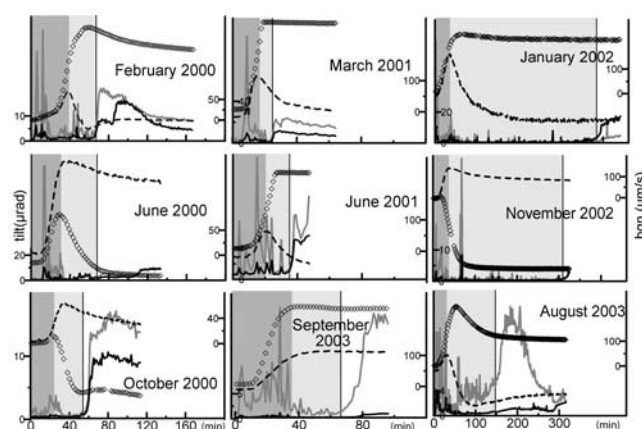

Figure 4. Comparison between the seismic bgn and the tilt signal. Black lines represent the seismic bgn at NSR for the northern eruptions and NTR for the southern eruptions. Grey lines represent the seismic bgn at the Bor, and black dash lines and diamonds represent respectively the radial tilt signal at SFR and Dsr stations. The dark and light grey areas are related to the two stages of the injection described in text.

presence of a single but anisotropic shallow magma chamber generating overpressures triggering the rupture of one or the other side of system. In any cases, a main magma chamber, located under the Dolomieu crater deeper than 200 to 800 meters a.s.l. (the depth of the seismic swarms), could feed the very shallow magma plumbing system. This main magma chamber has been suggested by the presence of a body with low velocity for P and even S waves just below sea level [*Nercessian et al.*, 1996].

[11] In the second phase, tilt vectors undergo a rotation indicating the beginning of a lateral injection of magma radiating away from the central area on the northern or southern flanks of the volcano (Figures 2 and 3). The inflation centre migrates in the direction of the future eruptive vents. In the same time, the seismic bgn decreases considerably at the summit stations due to the decrease of seismicity under the summit craters, and increases at the stations located at proximity of the dyke intrusion where few larger earthquakes occur but numerous microseismic events are recorded (Figure 4).

[12] A general deflation of the summit is recorded before the onset of the eruption. This deflation is related to the release of pressure under the summit as the dyke propagates to the flank. The seismic bgn increases again due to eruption tremor at the onset of the fissure eruption (Figure 4).

3.2. Speed and Duration of Injection

[13] The temporal detection of the dyke emplacement allows to estimate the duration and speed of magma migration (Table 1). Figure 5 shows that the durations of the vertical and lateral injections of magma correlate with the horizontal distance of the eruptive fissures from the summit. Considering that the vertical migration is defined by high seismicity and rapid summit inflation, the duration ranges from 7 to 20 minutes for eruptions which are located in the vicinity of the summit craters at a distance less than 1500 meters from the central zone and from 40 to 50 minutes for eruptions which are located at the base of the central cone or further away. For the eruptions we considered, if we make the assumption that there is no significant chemical or rheological change from a magma to another [*Semet et al.*, 2004], and that all the injections occur in the same wall rock (similar fracturing and resistance of rocks), the fluctuation of vertical durations suggests that magma start its ascent at different depths. The further the eruption takes place away from the summit, the longer the
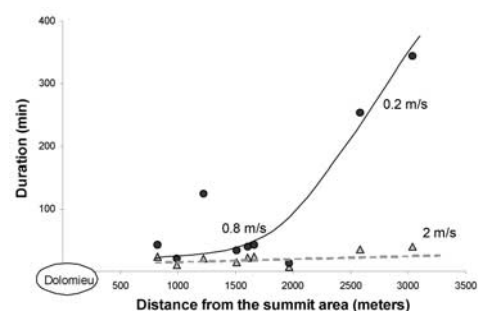

Figure 5. Duration of vertical (grey triangles) and lateral (black dots) magma injections at Piton de La Fournaise as a function of the distance of eruptive vents from the summit.
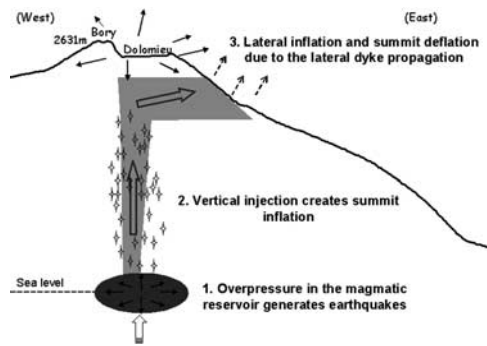
Figure 6. Conceptual model of the magma injection process before flank eruptions at Piton de La Fournaise. Stars indicate the location of some earthquakes occurring during the studied period.

duration of both lateral and vertical injections which may indicate a deeper root of the dyke. A deeper root of the feeding dyke allows a longer lateral migration before reaching the surface.

[14] Considering the time required for the magma to ascent from the bottom to the top of the volume where the seismic swarm is located, estimations of the mean vertical speed give a value of about 2 m/s (Figure 5). Lateral migration speeds of the dyke propagation within the cone ranges between 0.2 m/s and 0.8 m/s. As soon as intrusions propagate away from the cone, propagation speed seems to decrease (Figure 4). The migration speed of the magma remains in the same order or higher than documented in other volcanic edifices. In north Iceland, *Gudmundsson* [1995] estimates a speed of 0.4 to 1.2 m/s for several rifting events during the period of 1975 to 1986 on the Krafla. In Kilauea, *Okamura et al.* [1988], from tiltmeter data, estimates a speed of 0.15 m/s for the Pùu Òo eruption, and in Japan, *Ueki et al.* [1993] estimates from the propagation of earthquakes a speed of 0.003–0.11 m/s for the Teishi Knoll eruption. The high dyke propagation rates in the vicinity of Dolomieu crater can be explained by the dense network of radial and tangential fractures that offer preferential pathways for the magma intrusion to start its lateral migration. Dyke geometries and orientations depend mainly on the direction of surrounding stress field. A dyke injection leads to an eruption if the local stresses along the potential pathway are favourable for the propagation of magma-driven fracture up to the surface [*Gudmundsson and Brenner*, 2004]. In heterogeneous and fractured rocks, dyke propagation can be influenced by changes in the Young's modulus. A weaker Young's modulus tends to release the stresses around the tip of the fracture and guides the injection [*Gudmundsson*, 2002]. Thus, as soon as an ascending dyke meets a network of lateral fractures, it tends to divert and to migrate laterally to the flank, explaining the eruptive vent locations along two main rift zones and the third N120°E direction (Figures 1 and 3).

[15] At Kilauea volcano, where the rift zones are well developed, a significant seismic swarm in the rift zone preceded eruptions and was caused by the dyke emplacement [*Cervelli et al.*, 2002]. The region of the intrusion is characterised by high tensile stress due to the persistent dip rifting in the rift zone and by continued seaward sliding of the south flank. At Piton de La Fournaise, the rift zones consist exclusively of broad fragile areas highly fractured, which may explain the difference in the deformation and the seismic behaviour between the two volcanoes.

[16] The systematic study of these 9 dyke injections preceding flank eruptions indicates a steadiness of the feeding structures of the PdF eruptions with a recurrent global intrusive scheme implying the same structures, revealing a strong structural control exerted by the pre-existing fractures. Beyond this report, it also appears that this behaviour is similar to that described by *Toutain et al.* [1992] for the eruption of 1990, that occurred before the 1998 eruption interpreted as a major magma feeding phase of the summit complex of storage [*Battaglia et al.*, 2005].

4. Conclusion

[17] Magma movements into the central cone of Piton de La Fournaise can be well constrain by an analysis of the continuous recording of tilt and seismicity accompanying the seismic crisis before recent flank eruptions. This study allows us to propose a two phases recurrent model for the dynamics of magma injections at PdF soliciting the same structure in term of storage and plumbing system. A first, seismic, vertical injection at about 2 m/s starting of a magma chamber located at sea level under Dolomieu crater that evolves into a lateral dyke propagation guided by pre-existing fractures at 0.2–0.8 m/s.

References

Battaglia, J., and P. Bachèlery (2003), Dynamic dyke propagation deduced from tilt variations preceding the March 9, 1998, eruption of the Piton de la Fournaise volcano, *J. Volcanol. Geotherm. Res.*, *120*, 289–310.

Battaglia, J., V. Ferrazzini, T. Staudacher, K. Aki, and J.-L. Cheminée (2005), Pre-eruptive migration of earthquakes at the Piton de La Fournaise volcano (Réunion Island), *Geophys. J. Int.*, *161*, 549–558.

Bonaccorso, A., M. Aloisi, and M. Mattia (2002), Dike emplacement forerunning the Etna July 2001 eruption modeled through continuous tilt and GPS data, *Geophys. Res. Lett.*, *29*(13), 1624, doi:10.1029/2001GL014397.

Cervelli, P., P. Segall, F. Amelung, H. Garbeil, C. Meertens, S. Owen, A. Mikilius, and M. Lisowski (2002), The 12 September 1999 upper east rift zone dike intrusion at Kilauea volcano, Hawaii, *J. Geophys. Res.*, *107*(B7), 2150, doi:10.1029/2001JB000602.

Froger, J. L., Y. Fukushima, P. Briole, T. Staudacher, T. Souriot, and N. Villeneuve (2004), The deformation field of the August 2003 eruption at Piton de La Fournaise, Reunion Island, mapped by interferometry, *Geophys. Res. Lett.*, *31*, L14601, doi:10.1029/2004GL020479.

Fukushima, Y., V. Cayol, and P. Durand (2005), Finding realistic dike models from interferometric synthetic aperture radar data: The February 2000 eruption at Piton de La Fournaise, *J. Geophys. Res.*, *110*, B03206, doi:10.1029/2004JB003268.

Gudmundsson, A. (1995), The geometry and growth of dykes, in *Physics and Chemistry of Dykes*, edited by G. Baer and A. Heiman, pp. 23–34, A. A. Balkema, Brookfield, Vt.

Gudmundsson, A. (2002), Emplacement and arrest of dykes in central volcanoes, *J. Volcanol. Geotherm. Res.*, *255*, 279–298.

Gudmundsson, A., and S. L. Brenner (2004), How mechanical layering affects local stresses, unrests, and eruptions of volcanoes, *Geophys. Res. Lett.*, *31*, L16606, doi:10.1029/2004GL020083.

Lénat, J.-F., and P. Bachèlery (1990), Structure et fonctionnement de la zone centrale du Piton de La Fournaise, in *Le volcanisme de La Réunion*, edited by J.-F. Lénat, pp. 257–296, Cent. de Rech. Volcanol., Clermont-Ferrand, France.

Nercessian, A., A. Hirn, J.-C. Lépine, and M. Sapin (1996), Internal structure of Piton de La Fournaise volcano from seismic wave propagation and earthquakes distribution, *J. Volcanol. Geotherm. Res.*, *70*, 123–143.

Okamura, T. A., J. J. Dvorak, R. Y. Koyanagi, and W. R. Tanigawa (1988), Surface deformation during dike propagation, in *Pu'u 'O'o Eruption of Kilauea Volcano, Hawaii: Episodes 1 Through 20, January 3 1983, Through June 8 1984*, edited by E. W. Wolfe, *U. S. Geol. Surv. Prof. Pap.*, *1463*, 165–181.

Semet, M., T. Staudacher, and J. L. Joron (2004), Crystal-liquid relationships in the 1998–2003 products of Piton de La Fournaise, Reunion Island, paper presented at EGS-AGU-EUG Joint Assembly, Nice, France.

Toutain, J.-P., P. Bachelery, P.-A. Blum, J. L. Cheminee, H. Delorme, L. Fontaine, P. Kowalski, and P. Taochy (1992), Real time monitoring of vertical ground deformations during eruptions at Piton de la Fournaise, *Geophys. Res. Lett.*, *19*(6), 553–556.

Ueki, S., H. Hamaguchi, Y. Morita, T. Mishimura, and K. Kasahara (1993), Magma ascent process of the 1989 submarine eruption of Ito, Int. Assoc. of Volcanol. and Chem. of the Earth's Inter., Canberra, A. C. T., Australia.

————————

P. Bachèlery and A. Peltier, Laboratoire des Sciences de la Terre, Université de la Réunion, 15 avenue René Cassin, BP 7151, F-97715 Saint-Denis Cedex 9, France. (bachel@univ-reunion.fr; peltier@univ-reunion.fr)

V. Ferrazzini and T. Staudacher, Observatoire Volcanologique du Piton de la Fournaise, Institut de Physique du Globe de Paris, 14 RN3, le 27ème km, F-97418 La Plaine des Cafres, France. (ferraz@ipgp.jussieu.fr; thomas.staudacher@univ-reunion.fr)